Evidence of spin-glass ordering in sputtered $Y_{81.9}Tb_{2.6}Si_{15.5}$ metallic glasses

D. B. Gettman and D. J. Webb
Department of Physics, University of California, Davis, California 95616
(Received 15 November 1994)

We have measured the dc magnetization and ac susceptibility of sputtered amorphous $Y_{81.9}Tb_{2.6}Si_{15.5}$ films for evidence of spin-glass ordering. A splitting between zero-field-cooled (ZFC) and field-cooled curves at 4 K and a ZFC peak at 2.14 K indicate spin-glass ordering at these temperatures. A more careful magnetization study and a comparison with a Y-Gd-Si film of the same magnetic atom concentration reveals that this irreversibility is due to the magnetic anisotropy of Tb and correlations between neighboring spins. The ac susceptibility data indicates a spin-glass peak at 0.97 K. This value is compared to the transition temperatures for other amorphous spin glasses.

Amorphous metallic rare-earth spin glasses offer several advantages over the more familiar polycrystalline transition-metal spin glasses such as CuMn and AgMn for examining the three-dimensional to two-dimensional (3D) to (2D) crossover behavior of spin glasses.[1] First, various heavy rare-earth elements can be substituted on the rare-earth site to examine the effect of anisotropy on the spin-glass transition temperature and other spin-glass properties. Second, the rare-earth site can be diluted with yttrium or lanthanum to look at the spin-glass behavior in the limit of dilute magnetic atom concentration. These substitutions are not always possible in crystallite systems, but in amorphous systems do not result in significant structural changes. Third, the elastic mean free path of electrons is on the order of a lattice spacing[2] in a metallic glass so grain-boundary scattering is unimportant. Lastly, amorphous multilayers generally have smoother interfaces than polycrystalline multilayers due to lack of crystallite formation.[3] These last two advantages will become important in the limit of spin-glass layer thickness approaching zero.

One problem with the known metallic amorphous rare-earth spin glasses La-Gd-Au and GdAl is that they are incompatible with the use of Si as a nonmetallic decoupling layer between spin-glass layers due to interdiffusion.[4] This restricts the use of these materials to metallic decoupling layers. Our solution was to sputter deposit a new metallic amorphous spin glass based on the Y-Si eutectic composition $Y_{87}Si_{13}$.[5]

For the magnetic rare-earth element we chose Tb, primarily because of the work done on the magnetic, electrical and structural properties of a-$Tb_{87}Si_{13}$.[6,7] Since this alloy is a random anisotropy magnet, we need to have the magnetic atom concentration below the percolation threshold to form a spin glass. For example, the percolation threshold for a 3D nearest-neighbor Ising magnet on a fcc lattice is 20 at. %.[8] We choose a Tb concentration of 2.6 at. %, which would give a mean separation between Tb atoms of 0.65 nm.[9]

The Y-Tb-Si films were sputter deposited in a UHV chamber with base pressure $\sim 4\times10^{-8}$ torr. 99.999% Si, 99.9% Y, and 99.9% $Y_{97.1}Tb_{2.9}$ targets were dc magnetron cosputtered in an Ar pressure of 3 mTorr. The sputtering parameters were Si: $I=0.170$ A, $V=453$ V; Y: $I=0.950$ A, $V=313$ V; Y-Tb: $I=0.780$ A, $V=346$ V. The films were deposited at room temperature and the substrate temperature never exceeded 60 °C.

The films were simultaneously deposited on sapphire substrates for electron microprobe measurements and glass microscope slides for magnetic measurements. A 5 nm Cu layer was evaporated onto the glass slides in order to peel the sputtered film from the slide for magnetic measurements. All films were stored in a vacuum dessicator.

A buffer layer of 20 nm a-Si was deposited first so the magnetic film would adhere to the substrate, followed by a diffusion barrier of 30 nm a-$Y_{87}Si_{13}$ to prevent diffusion of the a-Si into the magnetic layer.[4] Then 500 nm of a-Y-Tb-Si was deposited, which will have the same spin glass transition temperature as a bulk spin glass from the results of Ref. 1. Another 30 nm a-Y-Si diffusion barrier was deposited on top of the magnetic layer, followed by an oxidation barrier of 20 nm a-Si. All sputtering rates had been determined previously with a Sloan DEKTAK 3030 step profilometer.

Electron microscope characterization of the film indicates that the composition of the Y-Tb-Si and Y-Si layers was $Y_{81.9}Tb_{2.6}Si_{15.5}$ and $Y_{85.0}Si_{15.0}$, respectively. Powder x-ray-diffraction scans of the films show no evidence of crystallite formation, with a 2θ full width at half maximum of the amorphous peak of 12.6°, which translates into a maximum crystallite size using the Scherrer formula[10] of 0.7 nm. No evidence of crystallization has been seen in films stored over a period of 2 years at room temperature in a vacuum dessicator.

The dc magnetization measurements were performed in a Quantum Design $MPMS_2$ superconducting quantum interference device (SQUID) magnetometer with a 1 T magnet. In the temperature range 295 to 5 K, the differential susceptibility was fit to a Curie-Weiss law. Data below 5 K were ignored because of the time relaxation evident in the films for temperatures below 4 K. To fit the data, we plotted χ^{-1} vs T (Fig. 1). From the Harris-Plischke-Zuckermann model,[11] the susceptibility

0163-1829/95/51(17)/11944(3)/$06.00

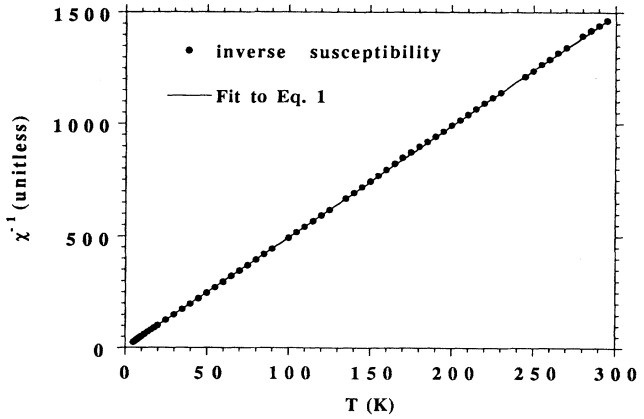

FIG. 1. Inverse volume susceptibility vs temperature. Y-Tb-Si 500 nm film. The line is at least-squares fit to Eq. (1) in the text. The fitting parameters used were $C=0.2030\pm3\times10^{-4}$ K, $\theta=0.840\pm0.2$ K, $\chi_0=2.01\times10^{-4}\pm1\times10^{-5}$.

can be fit to the form[8]

$$\chi=\chi_0+\tfrac{1}{2}C\left[\frac{1}{T^*-\theta}+\frac{1}{T^{**}-\theta}\right], \tag{1}$$

where $C=(N/V)\mu_B^2/3k_B$ is the Curie constant, θ is the Curie temperature, $T^*=Tf(D/T)$ and $T^{**}=Tf(-D/T)$, D is the random anisotropy constant and f is the function that describes the effect of random anisotropy on the susceptibility of the system.[9] We have made the assumption that there are an equal number of Tb atoms setting in sites of uniaxial and planar random anisotropy, which are the most probable symmetries for non-Kramers magnetic rare-earth atoms in an amorphous alloy.[12]

A value of $D=6.5$ K was taken from the value measured for a-$Tb_{87}Si_{13}$.[6] From neutron-scattering and magnetization data on Y dilution of heavy rare-earth elements, dilution does not affect the value of the anisotropy constants.[13,14]

The best fit values to Eq. (1) are $C=0.2030\pm3\times10^{-4}$ K, $\theta=0.840\pm0.2$ K, and $\chi_0=2.01\times10^{-4}\pm1\times10^{-5}$, which gives $\mu_{\text{eff}}=(9.89\pm0.1)\mu_B$. This value is higher than the free ion value for Tb, $9.72\mu_B$, and the difference may indicate electron-spin polarization.

Figure 2 shows the zero-field-cooled (ZFC) and field-cooled (FC) data at $H=50$ Oe. The separation between ZFC and FC curves occurs at 4 K, with the ZFC peak at 2.14 K. Notice that the peak is very broad and the FC curve does not exhibit spin-glass features.[15] A similar measurement on a Y-Gd-Si film with the same magnetic atom concentration (not shown) showed no evidence of irreversibilities. This indicates the relaxation behavior in the Y-Tb-Si film is due to time relaxation of correlated Tb spins over anisotropy energy barriers.

An equal time ZFC curve was generated by using magnetization measurements at different temperatures but the same time since the magnetic field stabilized at 50 Oe. An example is shown in Fig. 3. There is no peak in the data above 2 K. The ZFC peak in Fig. 2 is an artifact of

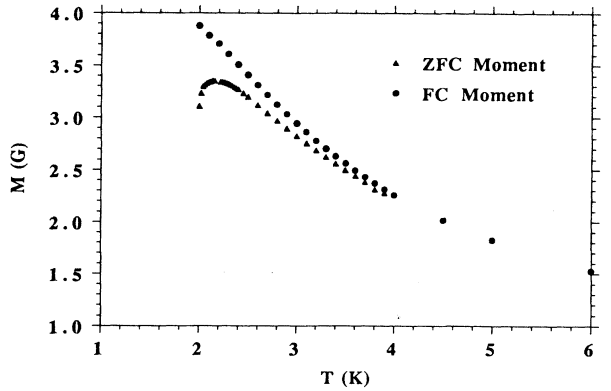

FIG. 2. Magnetization vs temperature, ZFC and FC curves. Y-Tb-Si 500 nm film. $H=50$ Oe.

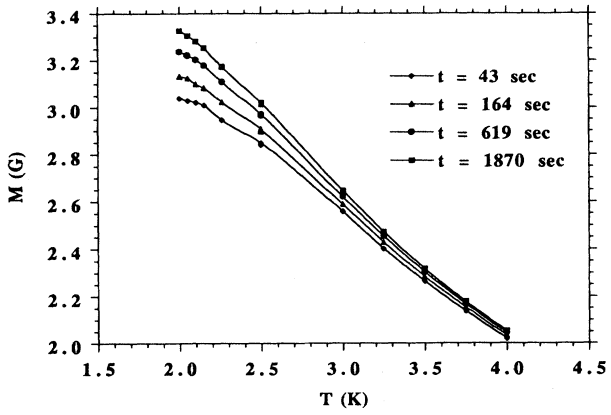

FIG. 3. Magnetization vs. temperature at equal times. Y-Tb-Si 500 nm film. $H=50$ Oe. The lines are guides to the eye.

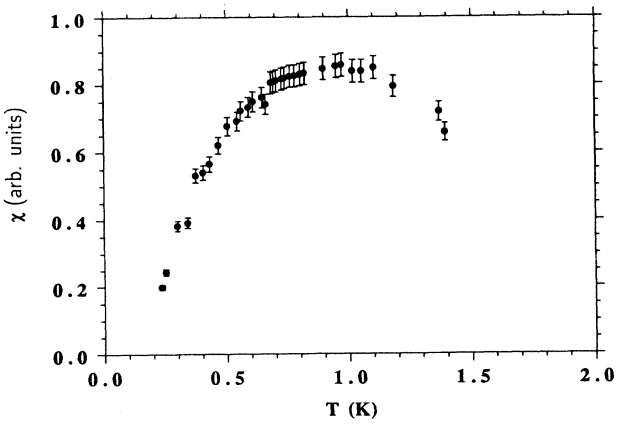

FIG. 4. In-phase susceptibility vs temperature. Y-Tb-Si 500 nm film. $f=104$ Hz.

taking the magnetic measurements at unequal times. As will be seen in the ac susceptibility data, the real spin-glass transition occurs at a lower temperature. Doing a simple cubic polynomial fit to the data, a peak is extrapolated to be at 1.63 K for $t=43$ sec, 1.50 K for $t=164$ sec, 1.35 K for $t=619$ sec, and 1.14 K for $t=1870$ sec, where t is the time since field stabilization.

Ac susceptibility measurements were taken in a SHE ^{3}He dilution refrigerator. The in-phase component of the ac susceptibility was measured at a frequency of 104 Hz with a driving field of $H_{\rm rms}=0.05$ Oe using a mutual inductance bridge. We were limited to the temperature range 8 mK–1.5 K because the dilution refrigerator develops temperature instabilities above 1.5 K.

Figure 4 is a plot of the ac susceptibility vs temperature. There is a broad peak centered at 1 K, with the width of the peak probably due to taking data while the temperature is changing in the region of the peak.

We have shown that a-Y-Tb-Si is a spin glass with a transition temperature of ~ 1 K. In comparison, the transition temperature is ~ 1.22 K for a-$Y_{31.4}Gd_{2.6}Al_{66}$ (Ref. 16) and a-$La_{77.4}Gd_{2.6}Au_{20}$.[17] If Tb was substituted for Gd in these alloys, $T_f \sim 0.8$ K due to the difference of total angular momentum and de Gennes factor of Tb vs Gd.[18] The difference in transition temperature may be due to the distance between rare-earth atoms in Y-Tb-Si vs Y-Gd-Al and La-Gd-Au.[19]

We would like to thank R. N. Shelton for the use of his x-ray diffractometer and SQUID magnetometer, P. Klavins for help with the magnetometer and diffractometer measurements, P. Schiffman for the electron microprobe measurements, L.R. Corruccini for the use of his dilution refrigerator and J. van der Noordaa for performing the ac susceptibility measurements. This work was supported by the NSF under DMR-8913855.

[1]G. G. Kenning, J. Bass, W. P. Pratt, Jr., D. Leslie-Pelecky, L. Hoines, W. Leach, M. L. Wilson, R. Stubi, and J. A. Cowen, Phys. Rev. B **42**, 2393 (1990).

[2]J. B. Bieri, A. Fert, G. Creuzet, and A. Schuhl, J. Phys. F **16**, 2099 (1986).

[3]E. Spiller, in *Layered Structures and Epitaxy,* edited by J. M. Gibson, G. C. Osbourn, and R. M. Tromp, MRS Symposia Proceedings No. 56 (Materials Research Society, Pittsburgh, 1986), p. 419.

[4]J. E. E. Baglin, F. M. d'Heurle, and C. S. Petersson, J. Appl. Phys. **52**, 2841 (1981).

[5]*Binary Alloy Phase Diagrams,* edited by T. B. Massalski (American Society of Metals, Metals Park, Ohio, 1987).

[6]P. Simonnin, R. Tourbot, B. Boucher, M. Perrin, and J. Vanhaute, Phys. Status Solidi A **98**, 551 (1986).

[7]P. Simonnin, R. Tourbot, B. Boucher, and R. Bellissent, J. Phys. F **17**, 559 (1987).

[8]John W. Essam, in *Phase Transitions and Critical Phenomena,* edited by C. Domb and M. S. Green (Academic, London, 1972), Vol. 2, p. 197.

[9]D. B. Gettman, Ph.D. thesis, University of California, Davis, 1994.

[10]B. D. Cullilty, *Elements of X-Ray Diffraction,* 2nd ed. (Addison-Wesley, Reading, MA, 1978).

[11]R. W. Cochrane, R. Harris, and M. J. Zuckermann, Phys. Rep. **48**, 1 (1978).

[12]J. Bieri, D. Bertrand, A. R. Fert, J. P. Redoules, and A. Fert, J. Magn. Magn. Mater. **80**, 246 (1989).

[13]H.-G. Purwins, E. Walker, B. Barbara, M. F. Rossignol, and P. Bak, J. Phys. C **7**, 3573 (1974).

[14]B. Barbara, Y. Berthier, R. A. B. Devine, and M. F. Rossignol, J. Phys. F **12**, 2625 (1982).

[15]K. Binder and A. P. Young, Rev. Mod. Phys. **58**, 801 (1986).

[16]A. P. Malozemoff, L. Krusin-Elbaum, and R. C. Taylor, J. Appl. Phys. **52**, 1773 (1981).

[17]S. J. Poon and J. Durand, Phys. Rev. B **18**, 6253 (1978).

[18]K. Baberschke, P. Pureur, A. Fert, R. Wendler, and S. Senoussi, Phys. Rev. B **29**, 4999 (1984).

[19]P. Villars and L. D. Calvert, *Pearson's Handbook of Crystallographic Data for Intermetallic Compounds* (American Society for Metals, Metals Park, Ohio, 1986).